SUPPLEMENTARY MATERIALS:

METHODS:

Mouse studies:

In vivo models: Each model had 8-10 mice per group of an experiment. Lipase injection into fat: The abdomen was shaved to facilitate visualization of the fat pads and cleaned with 70% ethanol. Five units of porcine pancreatic lipase [1] (Sigma-Aldrich, St. Louis, MO) in 0.2ml saline were injected percutaneously (25G needle) Q hourly into alternating (right and left) fat pads of ob/ob mice. When relevant, Orlistat (15mg/kg/injection) prepared as previously [2] was mixed in these. Mice were followed for 24 hours and euthanized then, unless they were noted to be moribund earlier, thus requiring euthanasia. The pulse distention, rectal temperature shown was measured at 12-16 hours of the first injection unless the mouse survived till 24 hours, when it was measured prior to euthanasia. Blood samples were collected at the time of necropsy. Oleic acid model: A single dose of oleic acid (0.3% body weight, intraperitoneally) was given to 8-12 week old CD-1 mice (Charles River laboratories) weighing 30-35 gms. The dose is based on oleic acid being the predominant fatty acid comprising ≈40% of visceral fat necrosis NEFA in previous human studies [3, 4], and visceral fat being an average of ≈3% of body weight (range 1-10%) in previous human studies [5], large parts of which can be necrosed during severe acute pancreatitis (e.g., Fig. 1 A2-A4). This oleic acid dose achieves the same oleic acid blood levels (Fig. 3A) as mice with severe pancreatitis (Figs. 7D, S11H), and humans with severe acute pancreatitis (Fig. 3J; which we noted after a blinded comparison). The intraperitoneal route is chosen to simulate the location of visceral fat necrosis. The mice were monitored twice daily for 3 days, and euthanized if they became moribund (average 48±13 hours). Blood parameters (Fig. 3) are those noted at the time of necropsy, and the pulse distention, rectal temperatures are from prior to euthanasia. Caerulein model*:* Lean or obese mice were given hourly intraperitoneal injections of caerulein (Bachem, 50mcg/kg), x14 doses daily for up to three consecutive days as described previously [2, 3]. This duration is necessary to simulate an attack

of severe pancreatitis in humans, which can last several days. IL12-18 model: Mice were given two consecutive intraperitoneal injections, at 24h intervals, of murine recombinant IL-12 (Peprotech, 150 ng/30g) and IL-18 (R&D Systems, 750 ng/30g) as described previously [6]. All animals received 2 ml saline subcutaneously Q12 hourly. Animals were followed for activity, rectal temperature and carotid pulse distention at 12 hours, and daily thereafter for up to 7 days or until they were moribund, whichever came first, at which time they were euthanized in a carbon dioxide chamber before harvesting blood and tissues.

Monitoring for organ failure: Carotid pulse distention (micrometers) was assessed with a collar sensor using the MouseOx oximeter (Starr Life Science, Pittsburgh, PA) at baseline, 12 hours, and daily thereafter to look for hypotension or shock. Rectal temperature, using a thermocouple probe and, tail vein blood sampling were also done. Mice were followed for 7 days or were euthanized when moribund. Blood, pancreas, visceral fat, and kidney and lung tissues were harvested to study various parameters of pancreatitis.

Injury parameters: Edema was measured as before [2, 7] by quantifying % water content measured as (wet weight-dry weight) x 100 / wet weight, and along with measuring percentage necrotic area (pancreas and fat), TUNEL positive cells (kidneys and lungs), and supportive serum cytokine and organ failure parameters. Histology, special stains (detailed below) and Immunohistochemical Studies: Pancreas, fat pad, kidney, and lung tissues were fixed with 10% neutral buffered formalin (Fisher Scientific), and embedded in paraffin and sectioned. Whole pancreas paraffin section (5 microns) slides stained by hematoxylin & eosin (H&E) were used to quantify pancreas necrosis, peri-fat acinar necrosis (PFAN, as described below) and acinar-to-ductal metaplasia (ADM), and slides stained by Von Kossa as previously described to quantify fat necrosis [4, 8]. For quantification purposes all pancreatic parenchymal areas stained by H&E were imaged using the PathScan Enabler IV slide scanner (Meyer Instruments, Huston, TX). Pancreatic acinar necrosis area (diffuse eosinophilic appearance of exocrine pancreas, with loss of cell morphological detail and outline), PFAN, i.e., parenchymal necrosis immediately

contiguous to areas of fat necrosis [4, 8], and area occupied by ADMs [9, 10] were measured as described previously. Briefly, total parenchymal area was measured in pixels, and percentage of total area necrosed/with metaplasia was calculated for each pancreas. In Von Kossa stained slides, intrapancreatic fat and necrotic fat (dark appearance of adipocytes) were measured and percentage of total fat necrosed was reported as a percentage of total fat for each pancreas [4, 8]. Analysis was done by a trained morphologist blinded to the sample (CDO or DLH).

Special stains: von-Kossa staining: This was done at the Mayo Clinic histology core facility, on paraffin sections as previously described [4, 8]. Von-kossa stains deposits of calcium or its salts [11], as occur with fatty acid saponification following pancreatitis causing fat necrosis [12] and fatty acid generation [13]. von-Kossa stain depends on silver nitrate replacing the calcium which has been reduced. This is seen as a black deposit under the microscope, and allows visualization of saponified fatty acids in and around fat necrosis. Masson's trichrome, Sirius red staining for fibrosis were done as per standard protocol of the histology core.
Terminal deoxynucleotidyl transferase dUTP nick end labeling (TUNEL) staining was done on paraffin sections of the lungs and kidneys to identify apoptosis, as described previously [2, 14]. Digital images of sections were captured with a digital microscope (Axio Imager.M2 or Axio Observer.Z1; Carl Zeiss) and quantified using a custom scripted ImageJ macro referred in supplementary Figure 7 of [15] as percentage of TUNEL-positive nuclei of all nuclei in tissue.

The horseradish-peroxidase immunohistochemical technique was used to detect myeloperoxidase (MPO) in paraffin embedded sections of lung tissue and to detect Pancreatic Lipase (PNLIP) in sections of pancreas and fat pad tissues. In brief, after deparaffinization and antigen epitope retrieval, tissues were incubated with a primary rabbit polyclonal antibody against MPO (dilution 1:50; AB9535, Abcam, Cambridge, MA) or PNLIP (1:200, ABS547, Millipore), followed by application of horseradish peroxidase-conjugated (dilution 1:1000; Millipore Corp) secondary antibody. Staining was completed with chromogen incubation with 3-

amino-9-ethylcarbazole substrate kit for peroxidase and hematoxylin QS nuclear counterstain (Vector Laboratories, Burlingame, CA).

Assays: All samples were included for assays and analyses unless the quantities were limited or there was an obvious error in procurement or processing.

Non-esterified fatty acid (NEFA) and visceral fat triglycerides analysis: Total plasma NEFAs and visceral fat triglyceride composition were assayed by gas chromatography at the Hormone Assay and Analytical Services Core (Vanderbilt University Medical Center, Nashville, TN) or as described previously[3, 4].

Cytokine and Chemokine Assays: The plasma cytokines and chemokine TNF-α, IL-6 and MCP-1 levels were assayed with a MILLIPLEX MAP Mouse Cytokine/Chemokine Magnetic Bead Panel assay (Millipore) according to the manufacturer's recommendations on a Luminex 200 System (Invitrogen, Carlsbad, CA) and analyzed using xPONENT software.

Biochemistry assays: Serum amylase, lipase, glycerol and blood urea nitrogen were measured according to the manufacturer's protocol (Pointe Scientific, Canton, MI). The lipase assay described in detail elsewhere[16] measures pancreatic lipase activity and is colipase and bile salt dependent. Lactate Dehydrogenase Assay was carried out with a cytotoxicity detection kit (Roche, Mannheim, Germany) according to the manufacturer's instructions. Blood glucose concentrations were measured by the glucose oxidase method using a FreeStyle glucose meter (Abbott Laboratories, Lake Bluff, IL).

Western blot analysis: Visceral fat pad or pancreas were homogenized in HEPES buffer containing proteases inhibitors cocktail (Complete, EDTA Free; Roche, Mannheim, Germany) and lysates boiled in 1X Laemmle sample buffer with SDS and beta-mercaptoethanol,

normalized for 1 mg/mL protein after protein estimation with a Pierce protein assay kit (Thermo Fisher Scientific, Rockford, IL) and loaded equally on 4-20%, or 10% Tris-Glycine gels for protein resolution. Proteins were transferred onto Immobilon PVDF membranes (EMD Millipore) and blocked in Tris-Buffered Saline (pH8.0) with 0.1% Tween20 containing 5% blocking grade blocker (Sigma).Western blot analysis was performed by incubation with primary antibodies detailed below: anti-adiponectin (1:1000, MAB10652, R&D Systems), Anti-amylase (1:20,000, A8273, Sigma-Aldrich, St. Louis, MO), anti-ATGL (1:1000; PA5-17436, Thermo Fisher Scientific), anti-chymotrypsin like (1:1000, MAB1476, EMD Millipore), anti-GAPDH (14C10) (1:2000, 2118S, Cell signaling, Danvers, MA), anti-PNLIP (1:10,000; [17], a kind gift from Dr. Mark Lowe, University of Pittsburgh), anti-PNLIPRP2 (1:1000; sc74853, SantaCruz Biotechnology, Dallas, TX)], anti-Na+K+ ATPase (1:4000, a6F, Developmental Studies Hybridoma Bank, University of Iowa), anti –Perilipin-1 (1:200, D418, Cell signaling technologies), anti Src (1:500, SC-18, SantaCruz Biotechnology, Dallas, TX), and anti-trypsin (1:200, AF3586, R&D systems), anti-vinculin (1:1000, sc73614, SantaCruz Biotechnology, Dallas, TX) and appropriate horseradish peroxidase labelled secondary antibodies at a concentration of 1:10,000 were used to detect the signal using ECL2 Western Blotting substrate (Thermo Fisher Scientific). Bands were visualized by chemiluminescence using electrogenerated chemiluminescence Pierce ECL Plus Western Blotting Substrate (Thermo Scientific).

Lipase, amylase and trypsin activity in tissue homogenates

Visceral adipose tissue or fat necrosis was homogenized on ice in a 1X PBS solution (final concentration of 137 mM NaCl, 10 mM Phosphate, 2.7 mM KCl, and a pH of 7.4). The homogenate was centrifuged at 14,000 × g for 10 min at 4°C and the resulting supernatant transferred to a new tube. Amylase and lipase (Pointe Scientific, Canton, MI), and total protein concentrations by Pierce BCA protein assay (Thermo Fisher Scientific) were performed

according to the manufacturer's protocol. Tests were performed on a GloMax Multimode Detection System (Promega, Fitchburg, WI). Trypsin activity was measured fluorometrically by using Boc-Gln-Ala-Arg-MCA (Peptides International, Louisville, KY) as the substrate according to the method of Kawabata et al[18]. The tissue homogenates from pancreatitis or diverticulitis VAT (in 10µl PBS, pH 7.4 per 1 mg of tissue) prepared using a glass teflon homogenizer, were centrifuged at 10,000g for 10 minutes. The infranatent under the upper layer of fat was taken and assayed. Briefly the infranatent was added into black 96-well microplate with a clear bottom (Corning, NY). Trypsin substrate was added into assay buffer containing 50mM Tris-HCl, 150 mM NaCl, 1 mM CaCL2 and 0.1 mg/ml bovine serum albumin. The mixture (195 µL) was added into the microplate and the fluorescence emitted at 440 nm after excitation at 380 nm was monitored. The enzyme activity was calculated as an increasing amount of fluorescent product formation per minute (ΔFlu/min =Fluorescence at that time – Previous minute Fluorescence). The normalization was done based on the amount of dsDNA present in the media (ΔFlu/min/dsDNA).

TLC protocol: Diverticulitis involved fat samples were homogenized in 10µl PBS per 1 mg of tissue. Homogenate was sonicated and 50µl (5mg) was taken for lipid extraction by Folch method. Similarly, pancreatic necrotic fluid was sonicated and 50µl taken for lipid extraction by Folch method. Lipid extracts were brought to a final volume of 150µl in $CHCl_3$. Woelm Silica gel G, 250 micron plates (Analtech, P16011) were prewashed in a 1:1 chloroform:methanol saturated tank, then dried and stored at 70°C until use. The TLC tank is saturated with running solvent (30:35:7:35, chloroform:ethanol:dH_2O:triethylamine) for 1 hour prior to use. 20µl involved fat and 100µl pancreatic necrotic fluid total lipid extracts were spotted on a line 1 inch from the bottom of a prewashed plate. The plate was placed in the saturated tank and ran until the solvent front reached ½ inch from the top. The plate was air dried (2-5 minutes), sprayed

thoroughly with primuline solution from an all glass atomizer and allowed to air dry once again before visualizing under UV light.

Recombinant proteins: Recombinant PNLIPRP2 was produced as described previously[16]. Plasmids for human *PNLIP*-mCherry (VB180328-1041npk) and human *PNLIPRP2* (VB181214-1159wpv) and its S148G mutant were constructed as described previously[16] using a mammalian gene expression vector under the CMV promoter (VectorBuilder Inc). Briefly, HEK 293T cells were transfected with Lipofectamine 3000(ThermoFisher Scientific, L3000008) according to the manufacturer's protocol. 24 hours after transfection, media was changed from DMEM containing 10% fetal bovine serum to serum-free DMEM and collected at 48 and 72 hours after transfection. Collected media was pooled and purified using HisPur Cobalt Resin according to the manufacturer's protocol (ThermoFisher Scientific, 89964). Purified proteins were concentrated in DPBS using Amicon Ultra-15 Centrifugal Filter Units (Millipore, C7715). Purity was confirmed by comassie blue staining.

Cell lines, culture experiments: All experiments in cell lines or primary cells were separately done 3-5 times.

3T3-L1 cell culture and use: 3T3-L1 cells were cultured in Preadipocyte Medium (PM-1-L1, ZenBio, Inc., USA) until 100% confluent in 20mm glass bottom 35mm dish compatible for confocal imaging (Cellvis, CA, USA) at 37oC in a humidified atmosphere (95% air and 5% CO2). Once cells were confluent, incubated another 48 hours in the Preadipocyte Medium. After that cells were differentiated for three days in Differentiation Medium (DM-2- L1, ZenBio, Inc., USA). Differentiated cells were maintained in Adipocyte Maintenance Medium (AM-1-L1, ZenBio, Inc., USA) for 3-4 for days until desired lipid droplets formed. Before starting, the cells for live cell imaging were serum starved for 1h and stained for lipid droplet with HCS LipidTOX™ Green neutral lipid stain (Ex/Em ~488/510, Thermo Fischer Scientific, USA). Then

cells were washed with the same serum free media for three times, followed by addition of purified PNLIP-mCherry, Co-lipase (5 µg, Sino Biological, USA), PLA2 (30 µg of 600-2400 units/mg stock, Sigma-Aldrich, USA) and LIVE/DEAD™ Fixable Far Red Dead Cell Stain (1X final concentration from 1000X stock, Ex/Em ~650/656, Thermo Fischer Scientific, USA) and live images were captured at 30 sec intervals for the indicated time periods using 63x Plan-Fluor oil immersion objective of laser scanning confocal microscope (LSM 800 ZEISS) and combined as a time lapse movie using Zen software.

The effect of PNLIPLRP2 on 3T3-L1 cells were monitored for 24 hrs by addition of purified PNLIPRP2-mCherry (360 µg, ~1000u/µg stock), after which images were taken after addition of LIVE/DEADTM Fixable Far Red Dead Cell Stain (1X final concentration from 1000X solution) and compared with the PNLIPRP2 untreated group.

Adipocyte and acinar cell isolation and use. Cell isolations were performed as described previously [4, 8, 19]. Pancreata were harvested from mice with the genetic background shown in the respective figure (e.g. C57/bl6 or PTL KO), and were immediately insufflated by 200U/ml collagenase type IV (Worthington Biochemical Corporation, Lakewood, NJ) in HEPES buffer pH 7.4 containing 10 mM HEPES, 130 mM NaCI, 5 mM KCl, 1 mM MgClz, 9 mM Na* pyruvate, 1 mM CaC12, 11 mM glucose, 0.1% bovine serum albumin, 0.01% soybean trypsin inhibitor and harvested as described previously [20]. This involved mincing with a with a sharp scissor, followed by shaking at 120 RPM at 37°C for a total of 40 minutes, after which they were triturated, strained and used. Viability was confirmed to >95% by trypan blue exclusion before use. For adipocytes, adipose tissue was minced with fine scissors in HEPES buffer containing 2% fatty acid free albumin and collagenase (375 U/mL) and incubated at 37 ^{o}C with shaking at 120 rpm for 40 min. After digestion, adipocytes were washed two times with 2% BSA/HEPES.

Isoproterenol stimulation was done as described previously[19]. 300 µL of adipocytes suspension were placed in a 24 well plate containing 700 µL of 1% BSA/HEPES with adenosine

deaminase (1 U/mL) (Worthington, Lakewood, NJ). The lipase inhibitors orlistat or atiglistatin (50μM) were then added to the relevant wells before adding the lipolytic activator isoproterenol. The adipocyte cell suspensions were then treated with 10 μM of Isoproterenol (Sigma) for 3hrs at 37 ^{o}C. After the incubation, 200 μL of infranatant were removed into microfuge tubes and used for the glycerol assay.

Acinar-adipocyte co-culture was done as previously described[4, 8]. Pancreatic acini were isolated as described previously[4, 8]. Acini and adipocytes were co-inclubated in a transwell system separated by a 3 micron mesh as shown in figure 4A and described previously [4, 8]. The medium contained 1% BSA/HEPES with adenosine deaminase (1 u/mL). The plates with the transwells were placed in an incubator shaker rotating at 150 RPM at 37°C for 6 hours. The medium was then removed and glycerol levels were measured in these. Acinar cell death was measured using propidium iodide (PI) uptake as previously described[4, 8]. Briefly, the upper chamber containing acini was removed inverted and washed with HEPES buffer to harvest the cells. The acini were stained with PI (BD Biosciences, San Jose, CA) at the end of the incubation period. Then the acini were washed with PBS and homogenized by motorized glass-teflon homogenizer on ice. The resulting homogenates were centrifuged and the supernatant was added into black 96-well microplate with clear bottom (Corning, NY), and the fluorescence emitted at 636 nm after excitation at 493 nm was monitored. The normalization was done based on the amount of dsDNA present in the homogenate. To identify of live or dead acini in a cell suspension we used Trypan Blue staining followed by light microscopy using a 10x objective. LDH leakage into the medium (as a percentage of 1% triton lysates taken as total), Calcium flux and mitochondrial depolarization were studied in acinar cells as described previously[4, 15, 21].

Supplementary Figures:

Fig. S1

Parameter	Acute pancreatitis	Acute diverticulitis	P value
Age	58.3±7.6	66.8±3.5	0.03
Sex (M:F)	4:4	4:4	NS
BMI	29.7±9.5	30.0±6.8	NS
Organ failure	5/8	0/8	0.03
Surgery day	59±32	62±60	NS

Fig. S1: Table comparing the demographics and clinical parameters of the acute pancreatitis and acute diverticulitis patients whose visceral adipose samples were chemically analyzed . Organ failure was defined at >48 hours of single or multiple organ failure as per the modified Marshall scoring system, which is the recommended method as per the Revised Atlanta Criteria. The surgery day refers to the interval between onset of disease and the time of surgery. BMI; Body mass index, NS; not significant.

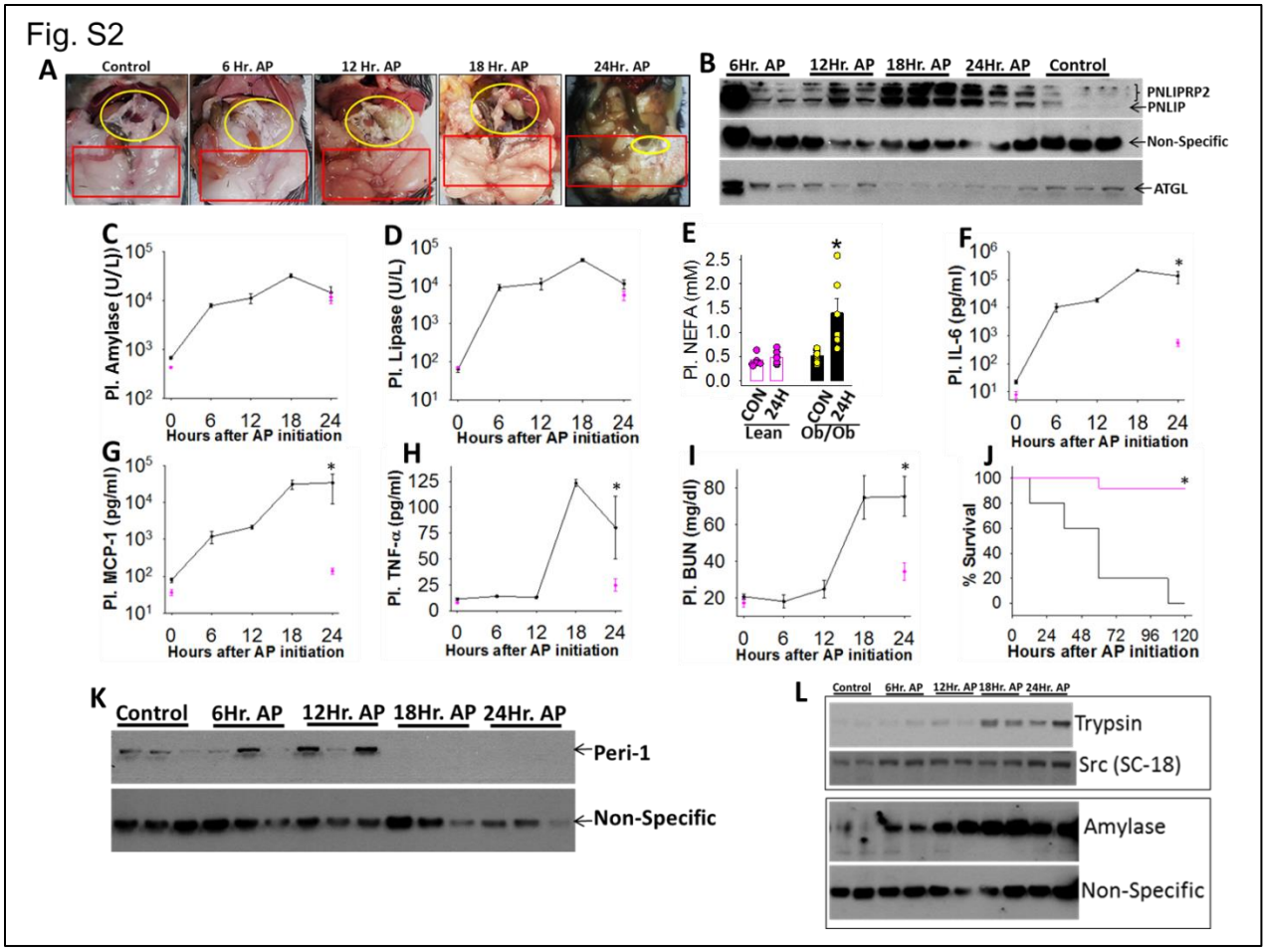

Fig. S2: Temporal course of the increase of pancreatic lipases in VAT, showing its correlation with fat necrosis, AP severity and loss of adipocyte proteins. . **A:** Gross appearance of the pancreas (yellow oval) and visceral fat (red rectangle) in situ in ob/ob mice over the time course of caerulein acute pancreatitis (from left to right), starting in controls. **B:** Western blot on the gonadal fat pads of these mice for ATGL, followed by stripping and probing for PNLIP and the non-specific band obtained at 25 KD after blotting for chymotrypsin (MAB1476, EMD Millipore, was used as a loading control. Time course of plasma (Pl.) amylase (**C**), lipase (**D**), IL-6 **(F**), MCP-1(**G**), TNF-α(**H**), BUN(**I**) in ob/ob mice (black line) with pancreatitis, along with baseline and 24 hour values for lean c57bl/6 mice with pancreatitis (in pink). **E**: Plasma NEFA in lean, ob/ob mice with no acute pancreatitis (control; CON) and after 24 hours of AP. The analyses are on 3-5 mice euthanized at each time point of the time line. **J**: survival curves of lean (pink) and ob/ob (black) mice with caerulein AP. * indicates a p <0.05 between the two groups. **K**: Western blot on the fat pads for Perilipin-1 (Peri-1), and the non-specific band obtained with MAB1476 (loading control on the same gel), of ob/ob control mice and those after different times of initiating caerulein pancreatitis**.** L: Western blot on the fat pads for trypsin, with Total Src (SC-18) shown as a loading control. Below shown is a contemporaneously run gel for amylase with the non-specific band obtained with MAB1476 used as a loading control. The names to the right side show the corresponding protein bands.

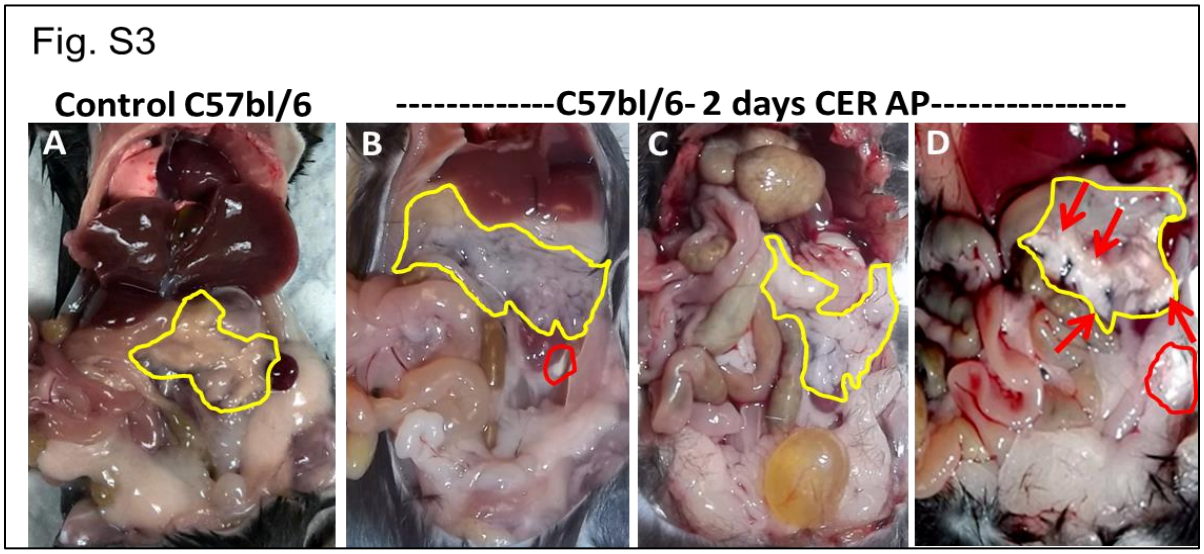

F**ig. S3: images of the peritoneal cavities of lean (C57bl/6) mice with and without caerulein AP. A** shows a control mouse without acute pancreatitis. **B-D** Show 3 mice with acute pancreatitis sacrificed **(B-C)** on the second day and the one mouse which died with acute pancreatitis (**D**). Yellow outlines the pancreas and red outlines the fat necrosis. Note the pancreas appearing edematous with acute pancreatitis, and **D** having significant fat necrosis in and around the pancreas. The red arrows and outlines in D show the only areas of fat necrosis that we could find in the whole series of lean mice (n=8) with caerulein pancreatitis. Mouse D was the only lean mouse that did not survive.

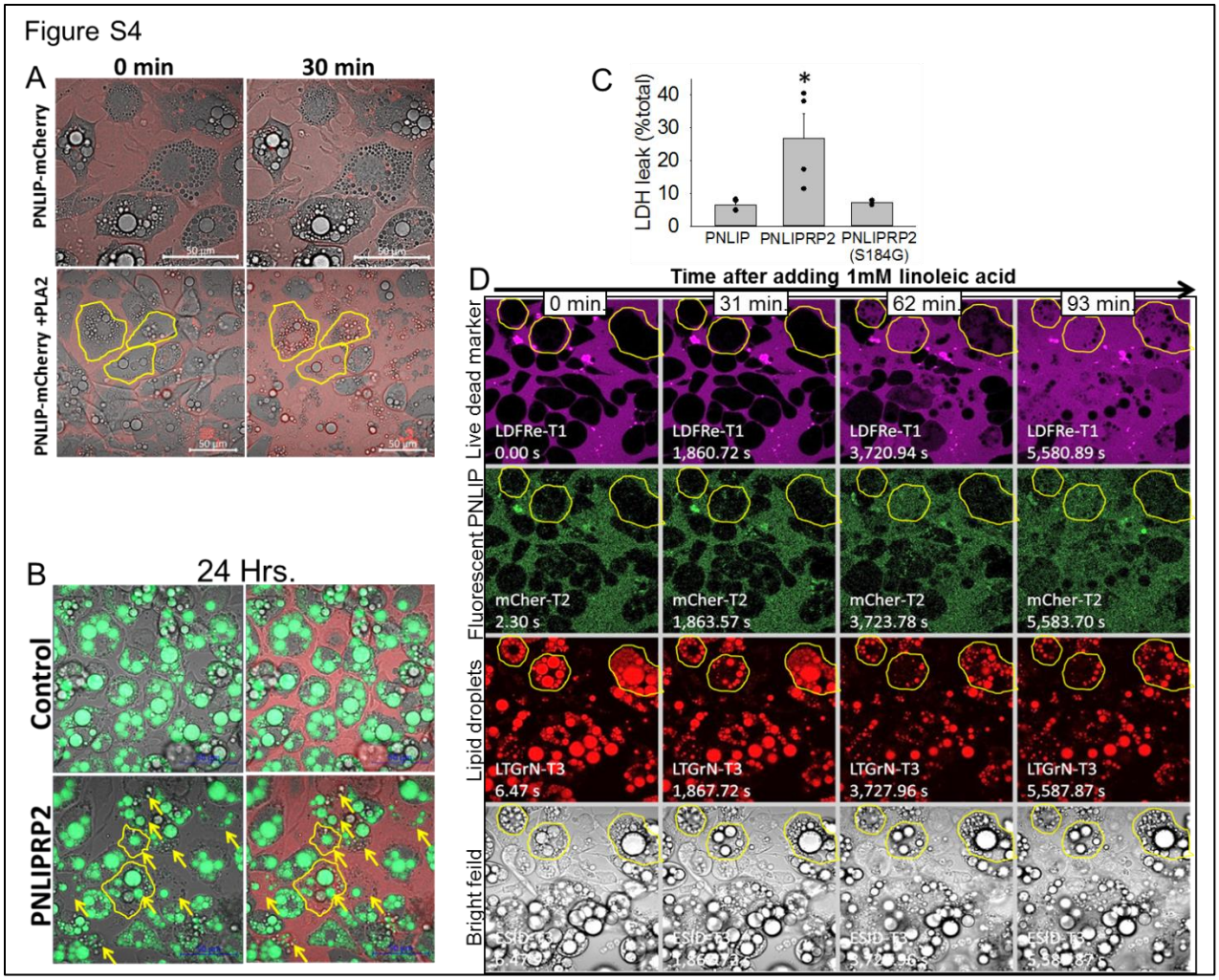

Fig. S4: Mechanisms by which adipocyte cell membranes may be compromised to allow entry of PNLIP into the cell: A shows PNLIP-mCherry added to 3T3-L1 cells (upper row) or PNLIP-mCherry added along with phospholipase A2 (PLA2; lower panel) as described in the methods. Note the outline of some of the cells showing a marked increase in uptake of the PNLIP-mCherry when added along with PLA2. **B:** Effect of adding PNLIPRP2 on the uptake of of LIVE/DEAD Fixable Far Red Dead Cell Stain (right panels). Lipid droplets are stained in green. The upper panel is untreated controls at 24 hours. The lower panel shows effect of PNLIPRP2 on uptake of the maker in cells with arrows, the outlines of some of which are shown. **C:** Cell injury measured as LDH activity in the medium (shown as a % of total LDH activity in cell homogenates) of HEK293T cells cultured with vectors expressing *PNLIP*, *PNLIPRP2*, and an inactive mutant of *PNLIPRP2* (S184G).* indicates a significant increase over PNLIP on ANOVA. Note that the S184G mutant of PNLIPRP2 causes less injury than PNLIPRP2 itself. **D:** Time series images of 3T3-L1 cells collected after different periods of exposure (shown on top) to linoleic acid (1mM). The upper row shows the LIVE/DEAD stain (purple), the second row shows fluorescent PNLIP (pseudo-colored green), the third row in red pseudo-color shows staining of neutral lipid with LipoTox®, and the bottom row shows the corresponding bright field images. In yellow outline are 3 cells showing the uptake of the live dead marker and fluorescent PNLIP, along with reduction in LipoTox® staining.

Figure S5

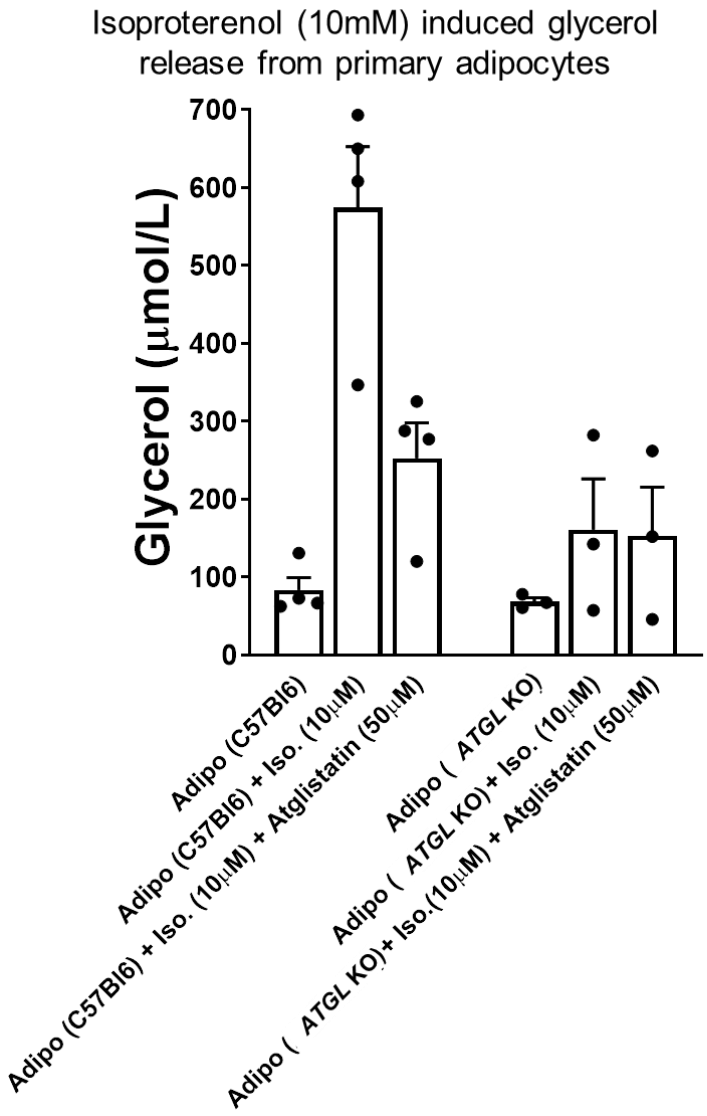

Fig. S5: Effect of the ATGL inhibitor (Atglistatin 50µM) and *ATGL* KO adipocytes on isoproterenol (Iso) induced glycerol release. Bar graphs showing the glycerol concentrations measured at the end of 3 hours incubation with isoproterenol (10µm) from 3-4 different experiments. Atglistatin when used was added 15-30 minutes before isoproterenol. * indicates a significant increase above control adipocytes [Adipo (C57bl6)], and †indicates a significant reduction compared to isoproterenol stimulated adipocytes.

Figure S6

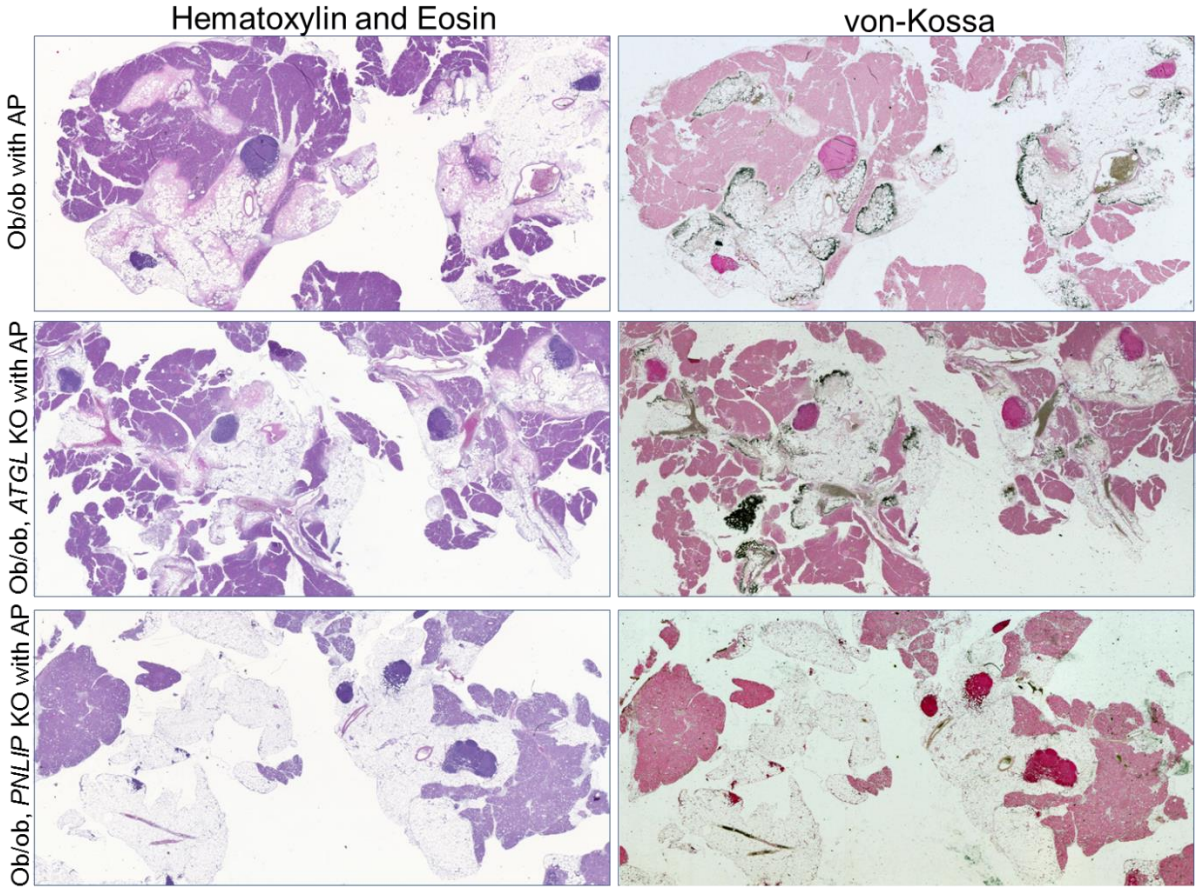

Fig. S6: Histologic appearance of serial formalin fixed paraffin embedded sections from caerulein pancreatitis and surrounding fat after Hematoxylin and eosin (H&E; Left) and von-Kossa staining (right) for calcium. Top row shows ob/ob mice, middle row shows ob/ob *ATGL* KO mice and bottom row ob/ob *PNLIP* KO mice. Note the diffuse pink color in the fat bordering the pancreas noted in H&E images, and corresponding positive (black) stain in the von-Kossa images. This signifies fat necrosis with calcification of the lipolytically generated NEFA. Note the paucity of these features in the images from ob/o *PNLIP* KO mice with pancreatitis.

Figure S7

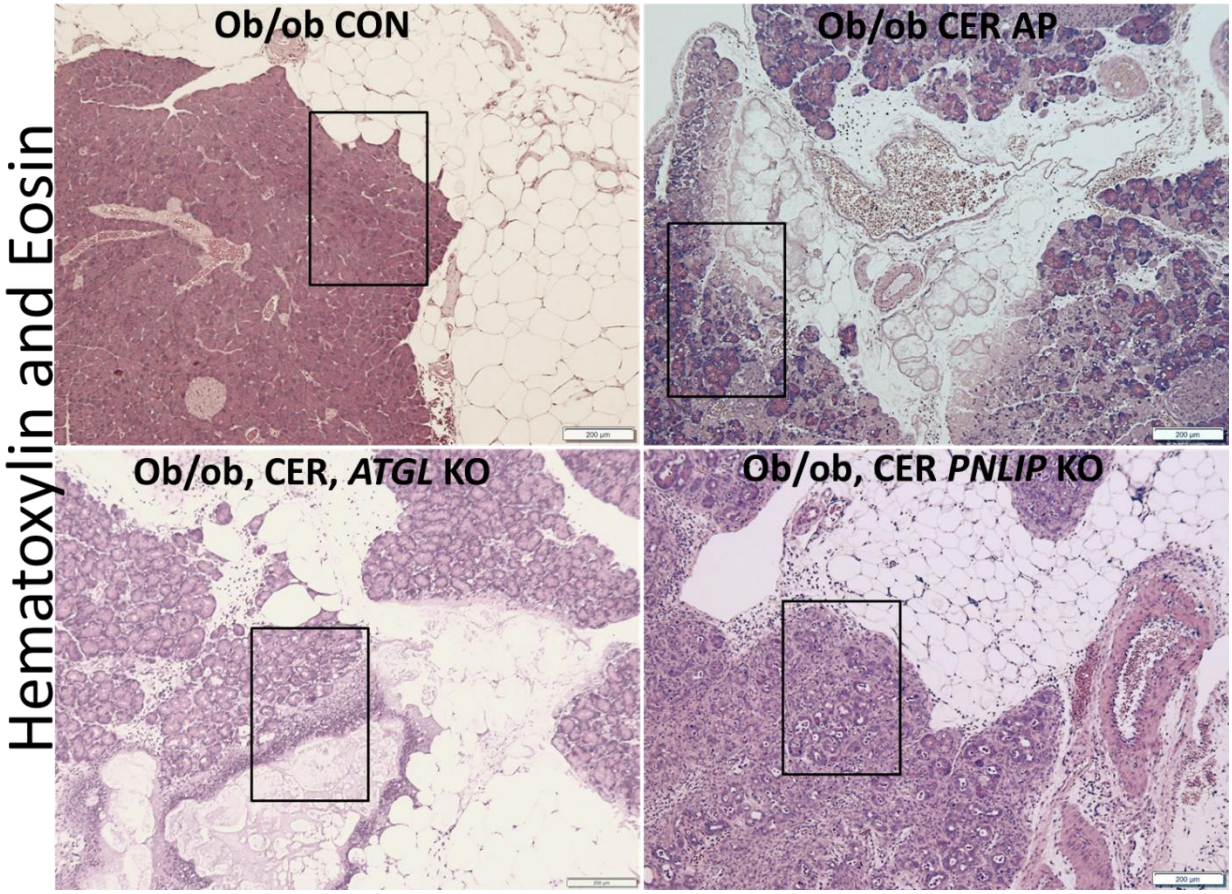

Fig. S7: Parent images of the sections shown in Fig. 6F. The rectangles are the areas that are shown in figure 6F. The scale bars are 200μM.

Fig. S8

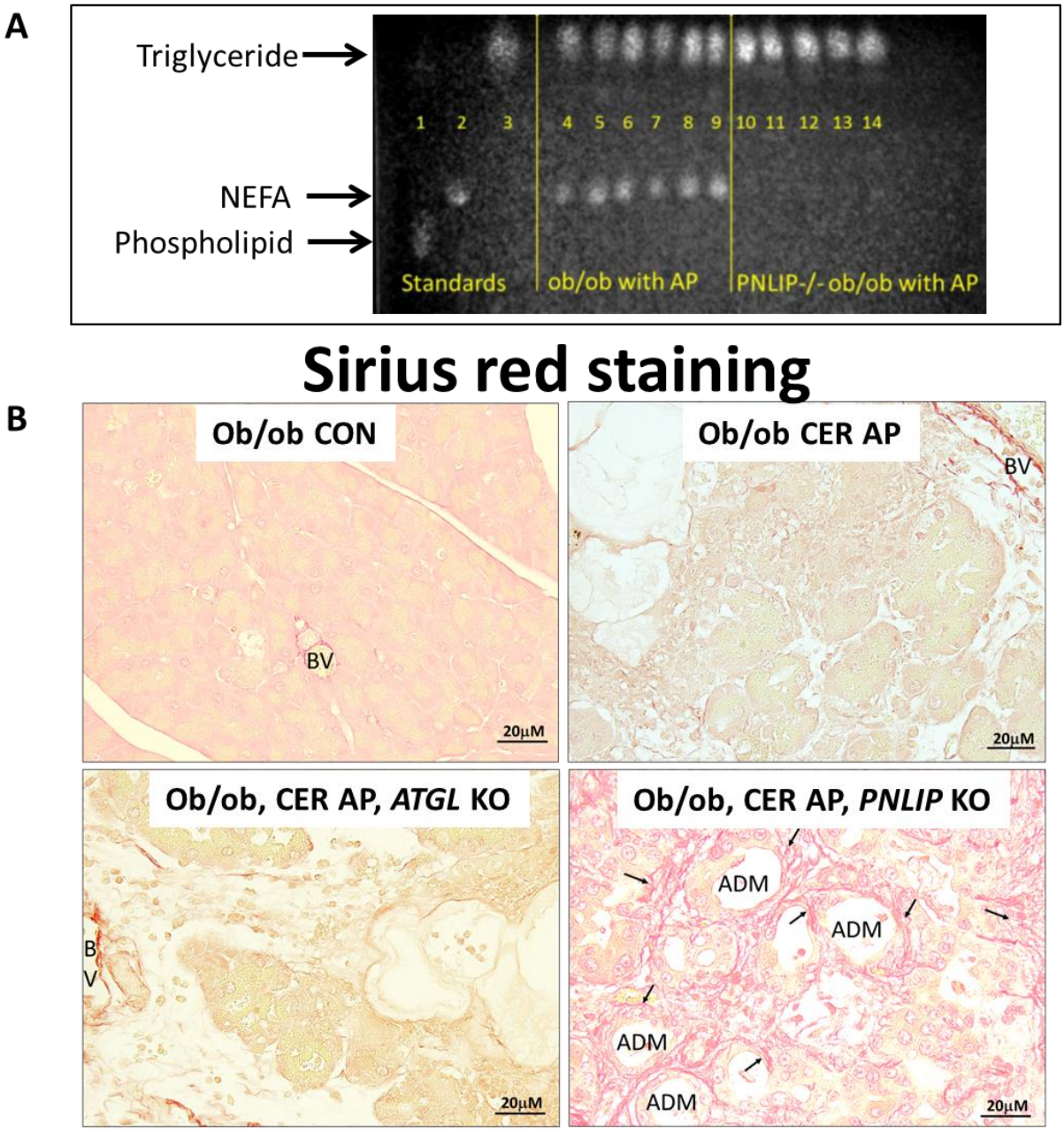

Fig. S8: A: Thin layer chromatography of fat pads of mice with pancreatitis (AP). To the left are the standards of the 3 lipid classes. B: Sirius red images of the pancreas showing fibrosis. Note that while under control and other conditions, the red strand like positive staining is only around blood vessels (BV), in the ob/ob *PNLIP* KO mice with caerulein pancreatitis (CER AP), there is a large increase in the red colored fibrosis (arrows) around the acini which have undergone acinar ductal metaplasia (ADM).

Fig. S9

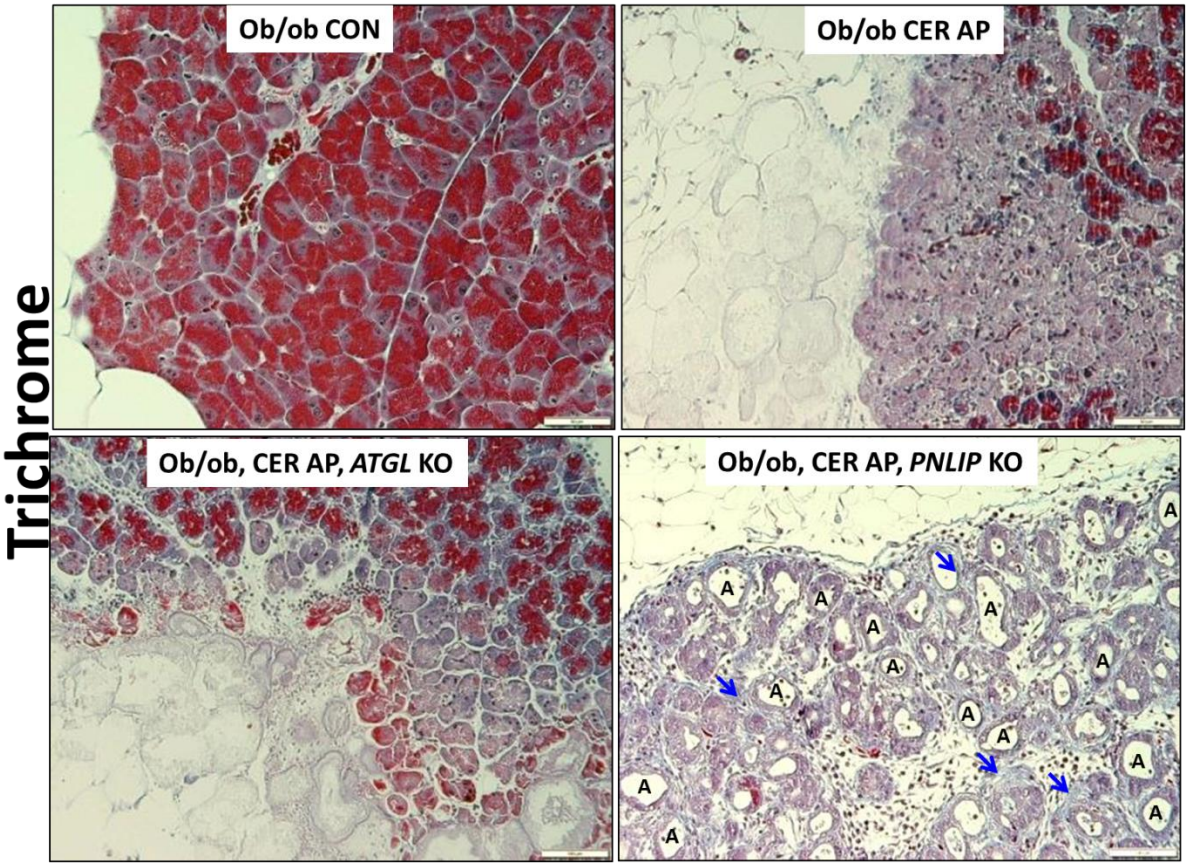

Fig. S9: A: Masson's trichrome stained images of the various groups. Note that in the ob/ob *PNLIP* KO mice with caerulein pancreatitis (CER AP), there is a large increase in the blue colored fibrosis (blue arrows) around the acini which have undergone acinar ductal metaplasia (A).

Fig. S10

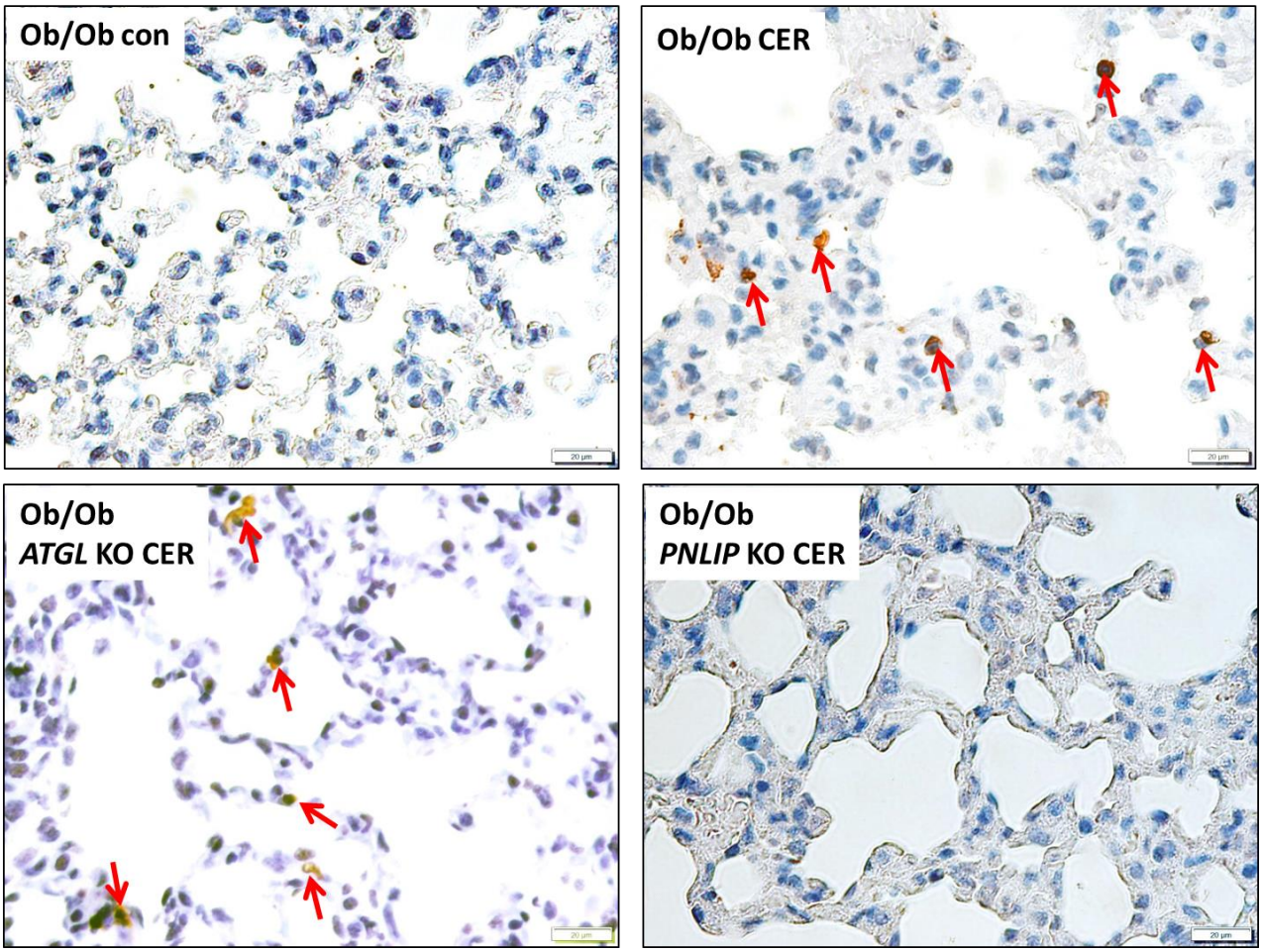

Fig. S10: TUNEL stained images of the lungs from different groups of mice. The groups represented in the image are mentioned in the left upper corner. The brown staining highlighted with red arrows shows the TUNEL positivity. Magnification was 40x.

Fig. S11

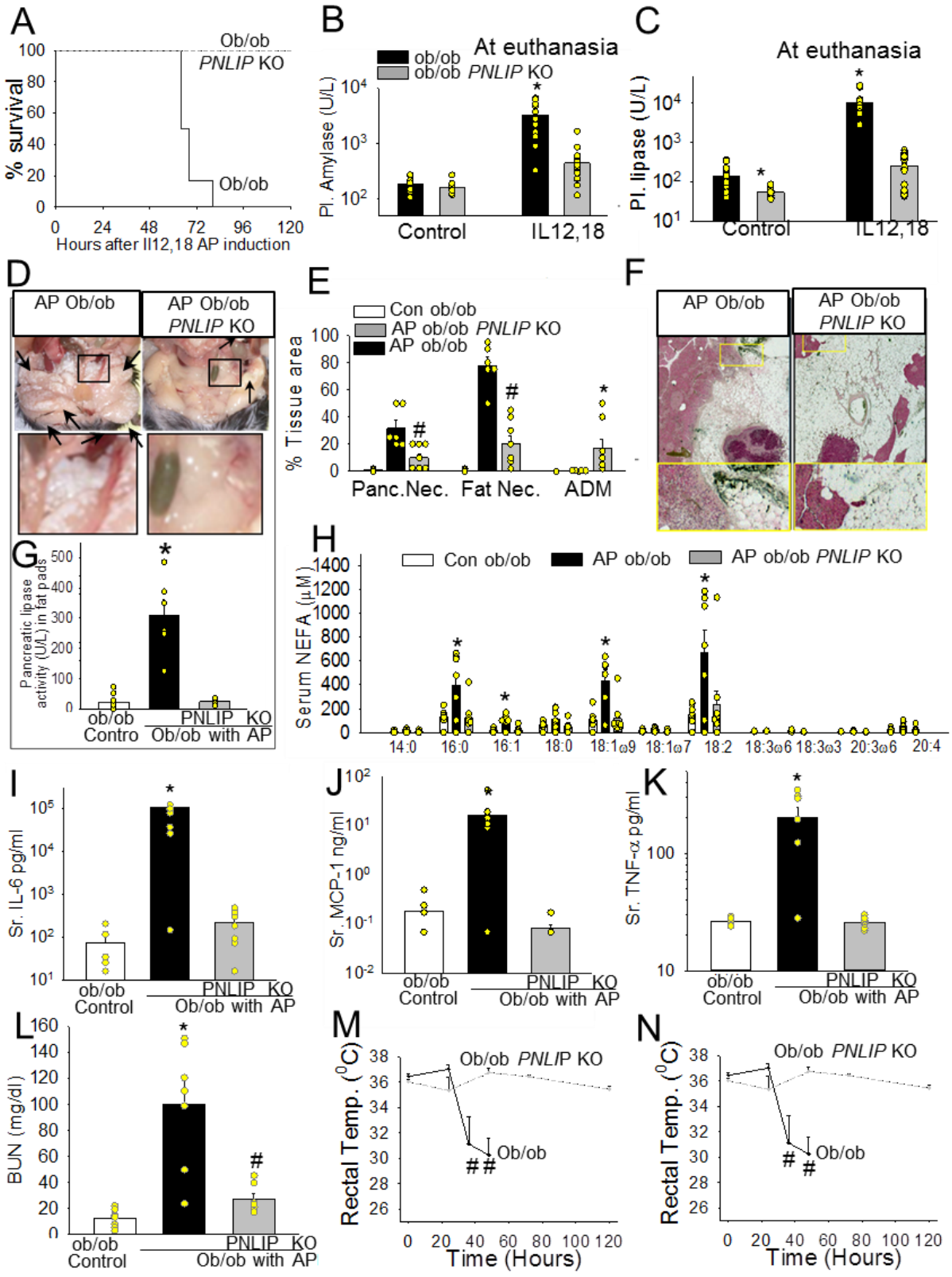
A
Ob/ob
PNLIP KO
Ob/ob
% survival
Hours after Il12,18 AP induction
B
At euthanasia
ob/ob
ob/ob PNLIP KO
Pl. Amylase (U/L)
Control
IL12,18
C
At euthanasia
Pl. lipase (U/L)
Control
IL12,18
D
AP Ob/ob
AP Ob/ob PNLIP KO
E
Con ob/ob
AP ob/ob PNLIP KO
AP ob/ob
% Tissue area
Panc.Nec.
Fat Nec.
ADM
F
AP Ob/ob
AP Ob/ob PNLIP KO
G
Pancreatic lipase activity (U/L) in fat pads
ob/ob Contro
PNLIP KO Ob/ob with AP
H
Con ob/ob
AP ob/ob
AP ob/ob PNLIP KO
Serum NEFA (μM)
14:0
16:0
16:1
18:0
18:1ω9
18:1ω7
18:2
18:3ω6
18:3ω3
20:3ω6
20:4
I
Sr. IL-6 pg/ml
ob/ob Control
PNLIP KO Ob/ob with AP
J
Sr. MCP-1 ng/ml
ob/ob Control
PNLIP KO Ob/ob with AP
K
Sr. TNF-α pg/ml
ob/ob Control
PNLIP KO Ob/ob with AP
L
BUN (mg/dl)
ob/ob Control
PNLIP KO Ob/ob with AP
M
Ob/ob PNLIP KO
Ob/ob
Rectal Temp. (°C)
Time (Hours)
N
Ob/ob PNLIP KO
Ob/ob
Rectal Temp. (°C)
Time (Hours)

Fig. S11: Comparison of ob/ob *PNLIP* KO (grey) and ob/ob mice (black) for IL12, 18 acute pancreatitis mediated parameters of pancreatic injury, fat necrosis, NEFA generation, inflammatory response, organ failure, and survival. A: Survival curve after acute pancreatitis induction. Circulating amylase (**B)**, and lipase levels (**C)** in control mice and at the time of necropsy after IL12, 18 acute pancreatitis. **D**: Appearance of the peritoneal cavity of ob/ob, ob/ob *PNLIP* KO mice with acute pancreatitis. Black arrows highlight the extent of fat necrosis and black rectangle shows the fat necrosis in proximity to the pancreas. **E**: Bar graph comparing the areas of pancreatic necrosis, fat necrosis, ADM in controls and the 2 groups with acute pancreatitis. * indicates a significant difference vs. the ob/ob mice with acute pancreatitis. **F:** von-Kossa staining of the pancreas and surrounding fat. Inset, with magnified view below compares the positive staining and necrosis in the bordering pancreas. **G**: Pancreatic lipase activity in the gonadal fat pads. **H:** Serum NEFA during acute pancreatitis and in control mice (white bar). * indicates a $P<0.05$ by ANOVA vs. controls. IL-6 (**I**), MCP-1 (**J**), TNF-α (**K**), BUN (**L**) in the various groups. * indicates a $P<0.05$ by ANOVA vs. controls. Trends of the carotid pulse distension (**M**) to measure shock, rectal temperature (**N**) to measure organ failure in the two groups. The dashed lines are *PNLIP* KO mice with acute pancreatitis. * indicates a $P<0.05$ by ANOVA vs. other groups, $^{\#}$ indicates a significant reduction in the ob/ob *PNLIP* KO mice vs. ob/ob mice with acute pancreatitis. Each group had 8-10 mice.

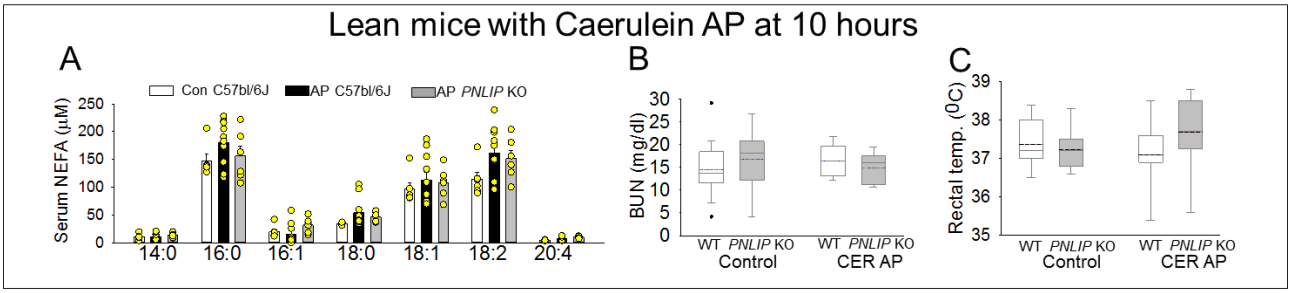

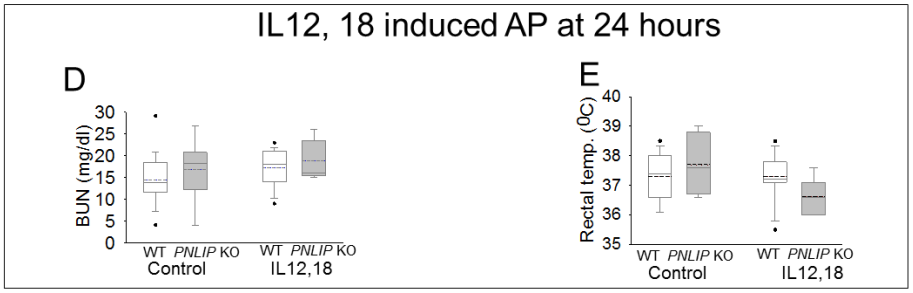

Fig. S12: Effect of *PNLIP* KO on caerulein acute pancreatitis (AP) in lean mice and early (24 hour) IL12, 18 induced pancreatitis. Serum NEFA (**A**), BUN **(B)** and rectal temperature **(F)** measured at the end of 10 hours of caerulein AP vs. controls . Note similar parameters in the two groups. Serum BUN (**D**), Rectal temperature **(E)** measured after 24 hours of the first Il12,18 injection. Note similar parameters in the two groups. Box plots depict mean (dashed line), median (solid line), 25th and 75th percentiles (2 boxes), 10th and 90th percentiles (whiskers), and outliers (dots).

Fig. S13

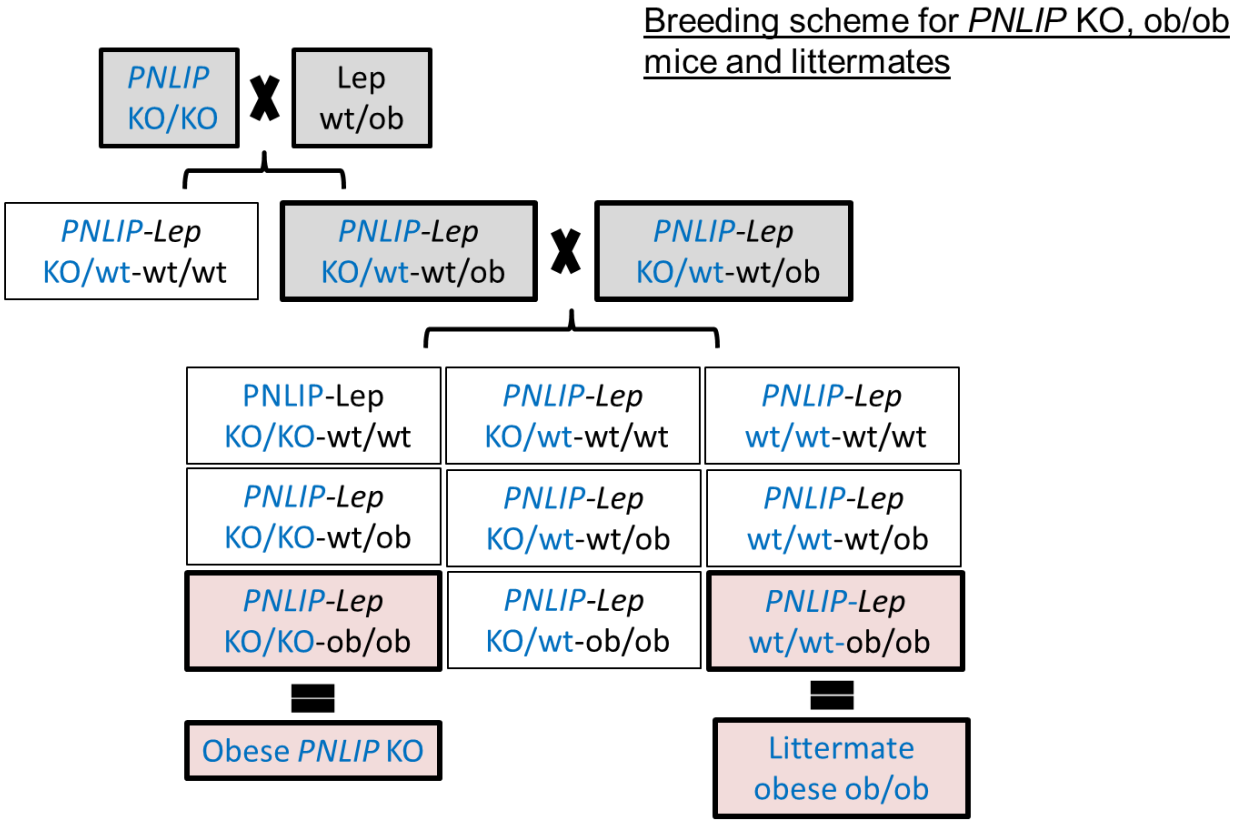

Fig. S13: Schematic showing the breeding strategy for *PNLIP* KO, ob/ob mice and littermates

Fig. S14

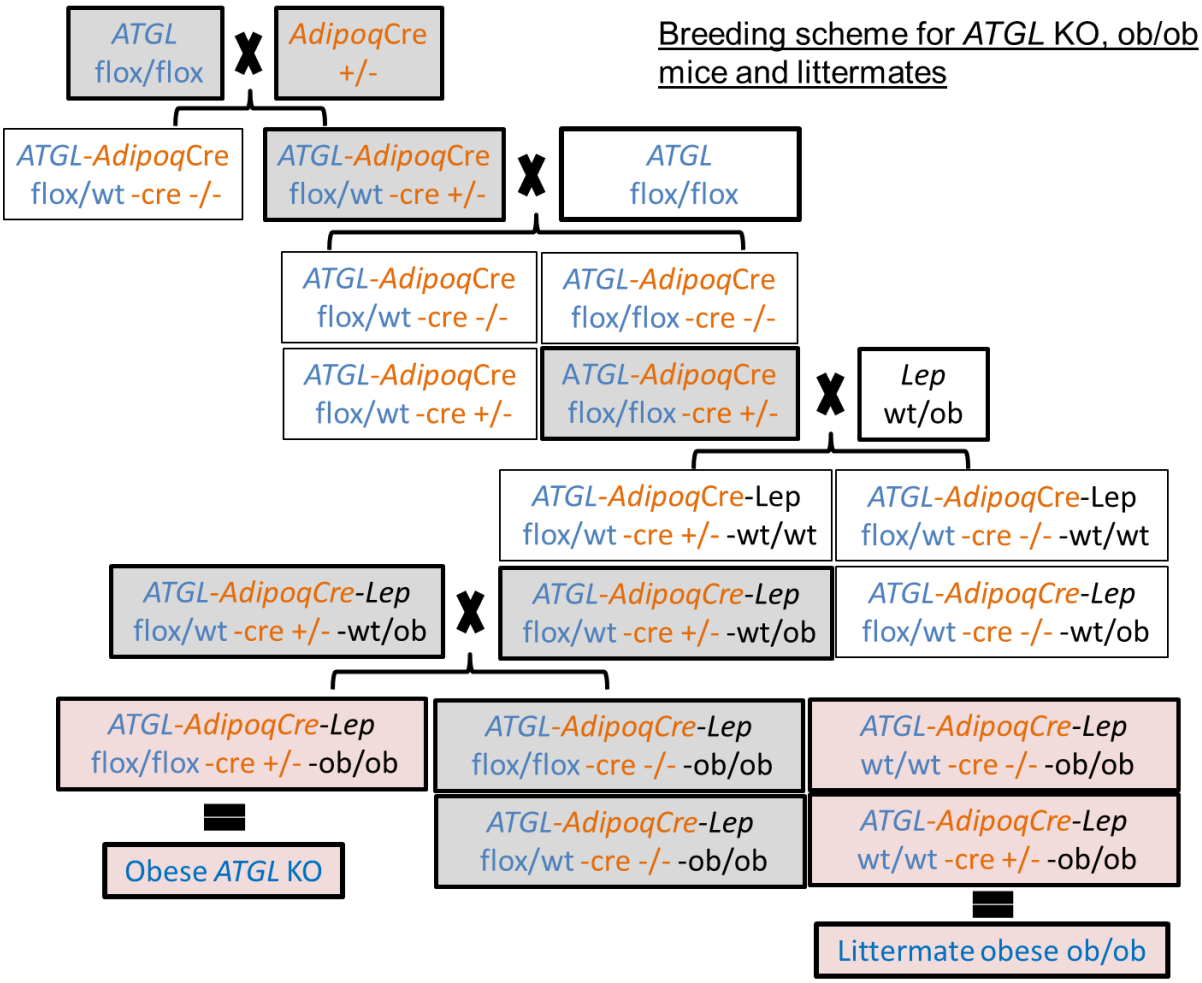

Fig. S14: Schematic showing the breeding strategy for *ATGL* KO, ob/ob mice and littermates

REFERENCES

1. Liu, X., et al., *Stereochemical Structure Activity Relationship Studies (S-SAR) of Tetrahydrolipstatin.* ACS Med Chem Lett, 2018. **9**(3): p. 274-278.
2. Patel, K., et al., *Lipolysis of visceral adipocyte triglyceride by pancreatic lipases converts mild acute pancreatitis to severe pancreatitis independent of necrosis and inflammation.* The American journal of pathology, 2015. **185**(3): p. 808-19.
3. Noel, P., et al., *Peripancreatic fat necrosis worsens acute pancreatitis independent of pancreatic necrosis via unsaturated fatty acids increased in human pancreatic necrosis collections.* Gut, 2016. **65**(1): p. 100-11.
4. Navina, S., et al., *Lipotoxicity causes multisystem organ failure and exacerbates acute pancreatitis in obesity.* Science translational medicine, 2011. **3**(107): p. 107ra110.
5. Camhi, S.M., et al., *The relationship of waist circumference and BMI to visceral, subcutaneous, and total body fat: sex and race differences.* Obesity, 2011. **19**(2): p. 402-8.
6. Sennello, J.A., et al., *Interleukin-18, together with interleukin-12, induces severe acute pancreatitis in obese but not in nonobese leptin-deficient mice.* Proc Natl Acad Sci U S A, 2008. **105**(23): p. 8085-90.
7. Orlichenko, L., et al., *ADP-ribosylation factor 1 protein regulates trypsinogen activation via organellar trafficking of procathepsin B protein and autophagic maturation in acute pancreatitis.* The Journal of biological chemistry, 2012. **287**(29): p. 24284-93.
8. Acharya, C., et al., *Fibrosis Reduces Severity of Acute-on-Chronic Pancreatitis in Humans.* Gastroenterology, 2013. **145**(2): p. 466-75.
9. Ding, L., et al., *Glycogen synthase kinase-3beta ablation limits pancreatitis-induced acinar-to-ductal metaplasia.* J Pathol, 2017. **243**(1): p. 65-77.
10. Bhanot, U.K. and P. Moller, *Mechanisms of parenchymal injury and signaling pathways in ectatic ducts of chronic pancreatitis: implications for pancreatic carcinogenesis.* Lab Invest, 2009. **89**(5): p. 489-97.
11. Wang, X., et al., *Bone marrow stem cells-derived extracellular matrix is a promising material.* Oncotarget, 2017. **8**(58): p. 98336-98347.
12. Herbert, F., *Pancreatic Fat Necrosis: A Chemical Study.* Br J Exp Pathol, 1928. **9**(2): p. 57-63.
13. Keen, C.E., et al., *Fat necrosis presenting as obscure abdominal mass: birefringent saponified fatty acid crystalloids as a clue to diagnosis.* J Clin Pathol, 1994. **47**(11): p. 1028-31.
14. Noel, P., et al., *Peripancreatic fat necrosis worsens acute pancreatitis independent of pancreatic necrosis via unsaturated fatty acids increased in human pancreatic necrosis collections.* Gut, 2014.
15. de Oliveira, C., et al., *Multimodal Transgastric Local Pancreatic Hypothermia Reduces Severity of Acute Pancreatitis in Rats and Increases Survival.* Gastroenterology, 2019. **156**(3): p. 735-747 e10.
16. Khatua, B., et al., *Carboxyl Ester Lipase May Not Mediate Lipotoxic Injury during Severe Acute Pancreatitis.* Am J Pathol, 2019.
17. Cotton, P.B., et al., *Rome IV. Gallbladder and Sphincter of Oddi Disorders.* Gastroenterology, 2016.
18. Kawabata, S., et al., *Highly sensitive peptide-4-methylcoumaryl-7-amide substrates for blood-clotting proteases and trypsin.* Eur J Biochem, 1988. **172**(1): p. 17-25.
19. Viswanadha, S. and C. Londos, *Determination of lipolysis in isolated primary adipocytes.* Methods Mol Biol, 2008. **456**: p. 299-306.

20. Powers, R.E., et al., *Diminished agonist-stimulated inositol trisphosphate generation blocks stimulus-secretion coupling in mouse pancreatic acini during diet-induced experimental pancreatitis.* J Clin Invest, 1986. **77**(5): p. 1668-74.
21. Patel, K., et al., *Fatty Acid Ethyl Esters Are Less Toxic Than Their Parent Fatty Acids Generated during Acute Pancreatitis.* Am J Pathol, 2016. **186**(4): p. 874-84.